Combined diffusive shock and shear acceleration in astrophysical jets

V.N.Zirakashvili, V.S.Ptuskin, S.I.Rogovaya
IZMIRAN

Cosmic ray spectrum

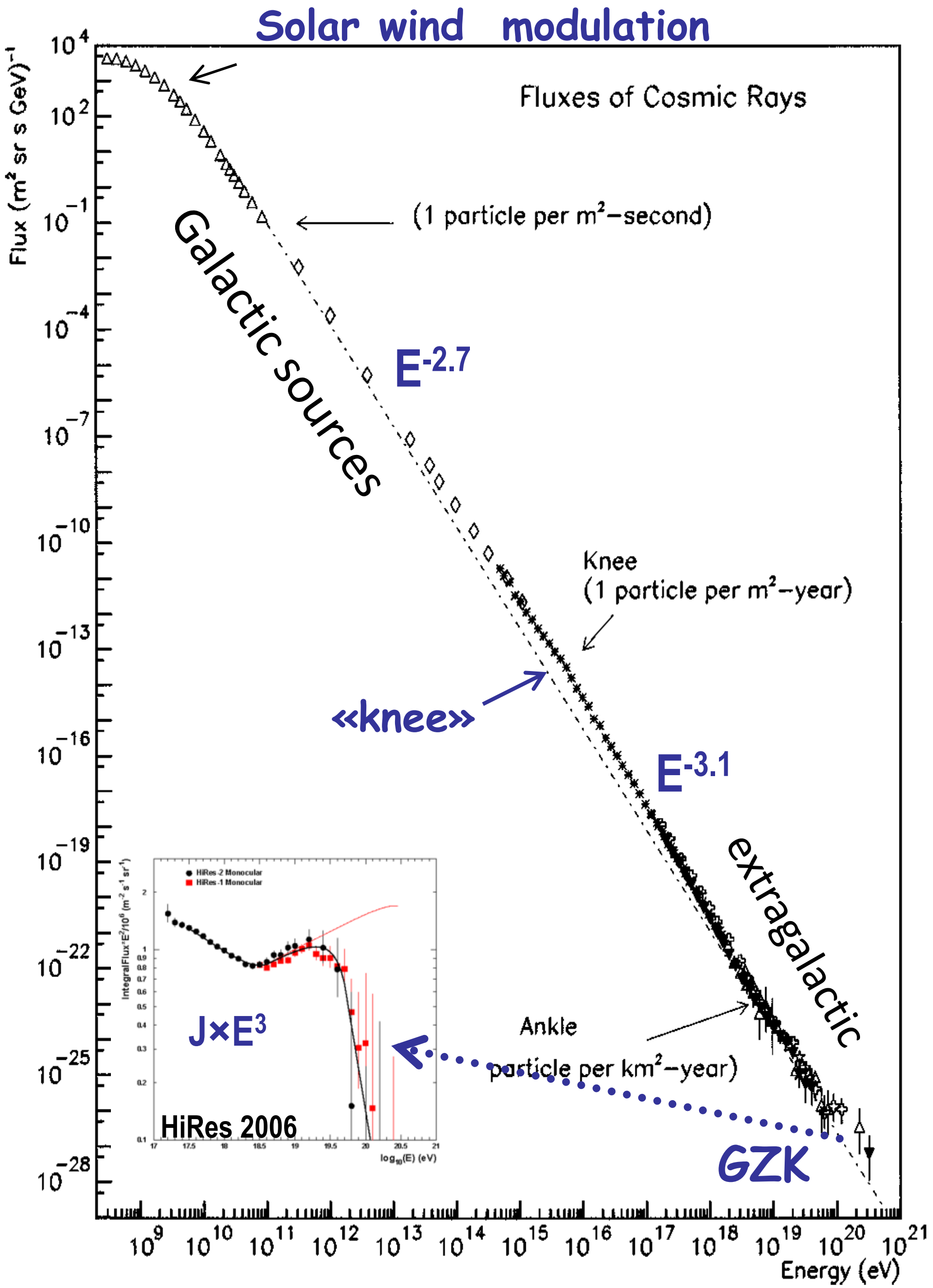

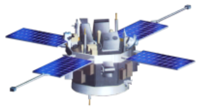

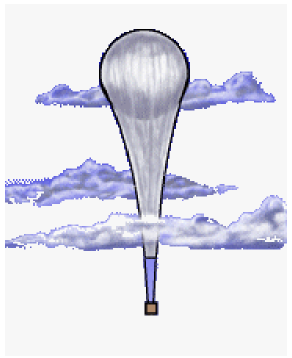

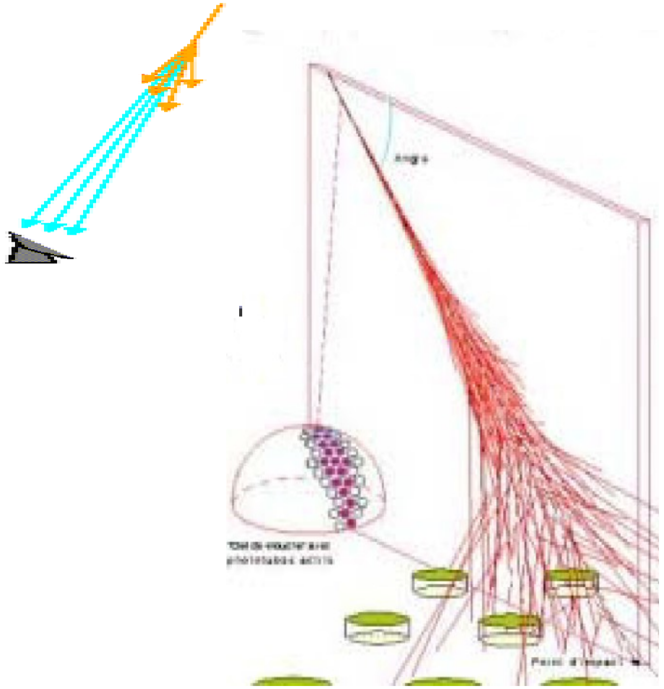

Particle acceleration in relativistic jets

$$E_{\max} = 1.7 \cdot 10^{19}\mathrm{eV}\ Z\beta^{1/2}\left(\frac{L_{\mathrm{mag}}}{10^{44}\mathrm{erg\ s^{-1}}}\right)^{1/2}$$

(Caprioli 2015) Reacceleration of CR particles - explains enrichment by heavy nuclei

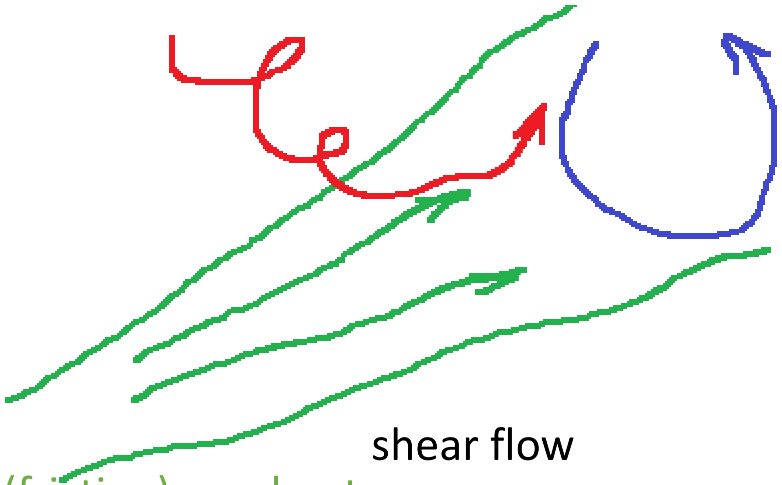

Torroidal magnetic field

shear flow

Shear (friction) acceleration
Berezhko 1981

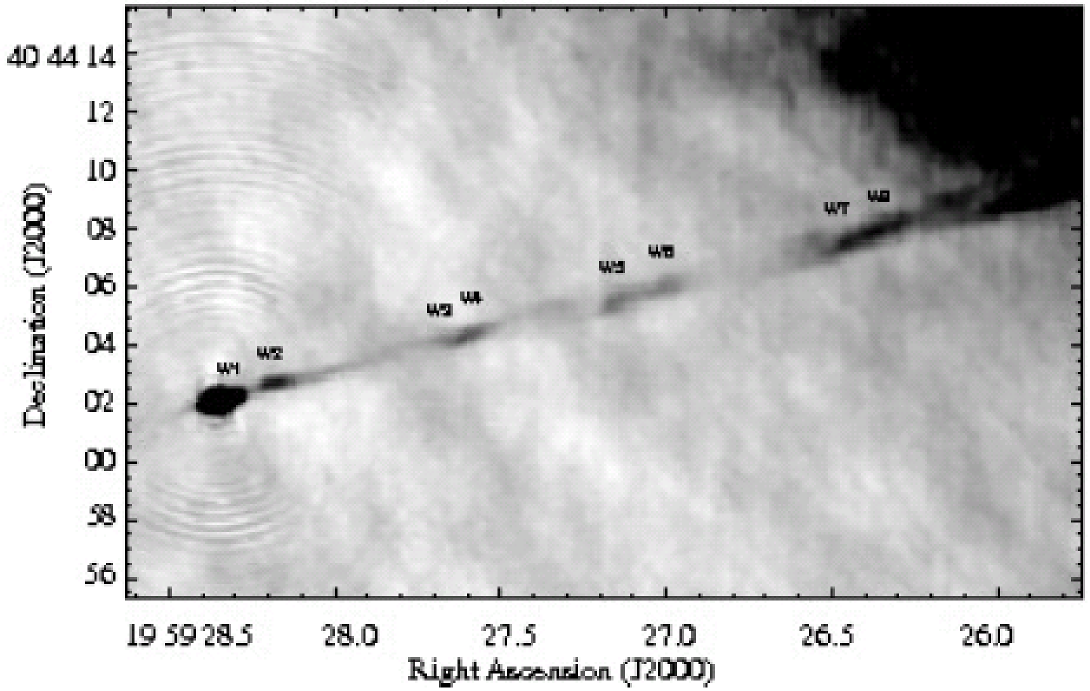

Figure 2. The inner jet of Cygnus A observed at 5 GHz. Note the weak emission between W1 and W2 which extends about half way to W3. Thereafter, there there are only hints of smooth emission between the jet knots, which become brighter from W7 onwards. The jet seems straight, but note the possible bend between W3 and W4. W7 and W8 are the first jet knots in what we call the 'outer jet'.

Cygnus A in radio, X-rays and optics (Blandford et al. 2019)

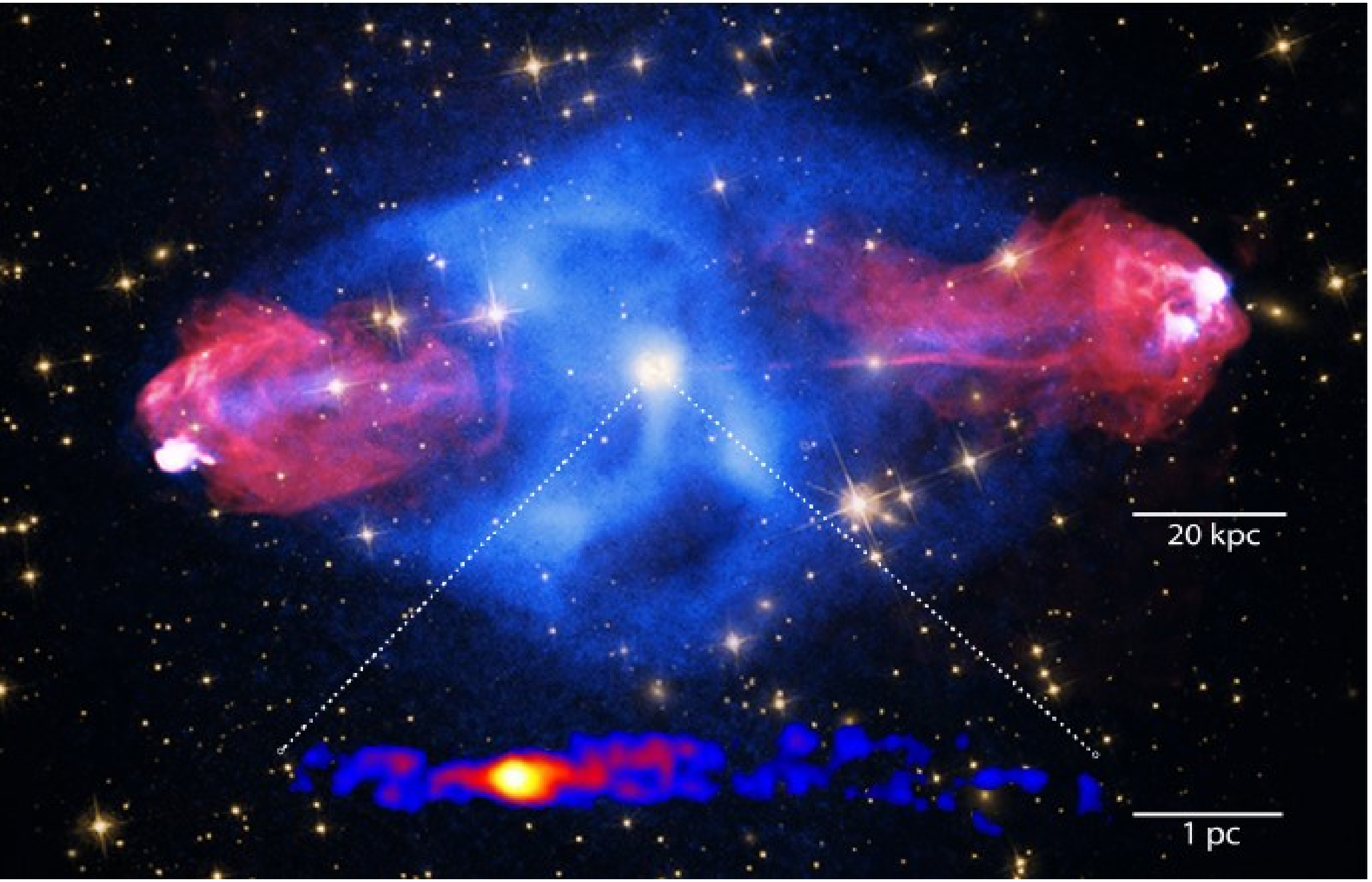

Hydrodynamical modeling of jets (Seo et al. 2021)

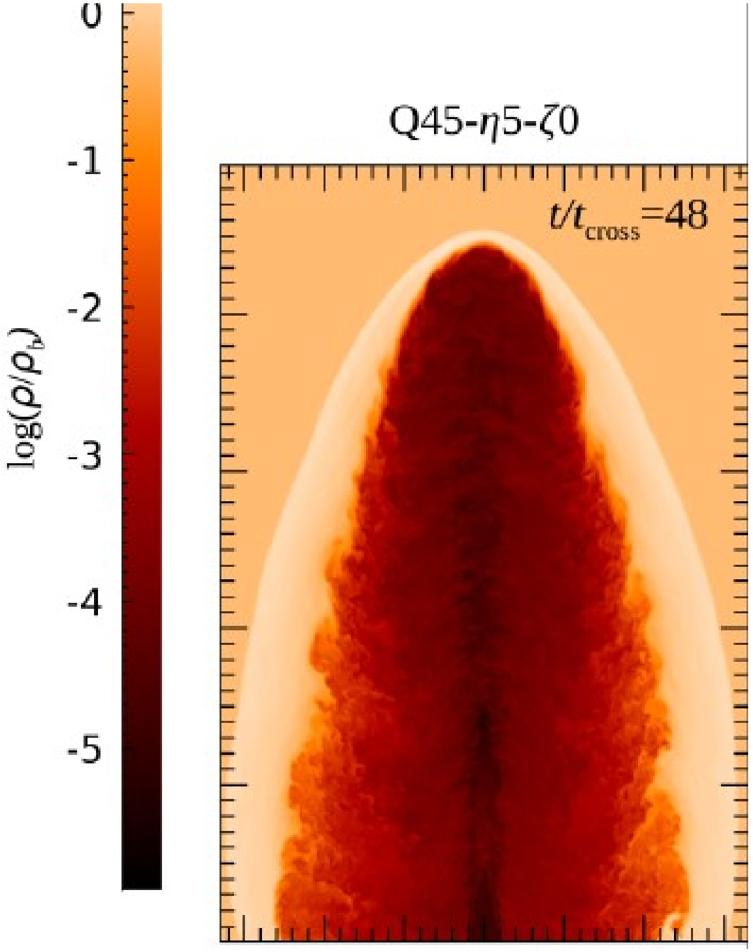

3 components of accelerated particles
(Zirakashvili et al. 2023)

$$q(\epsilon, A) \propto k(A)\epsilon^{-\gamma} \exp\left(-\frac{A\epsilon}{Z\epsilon_{\max}}\right)$$

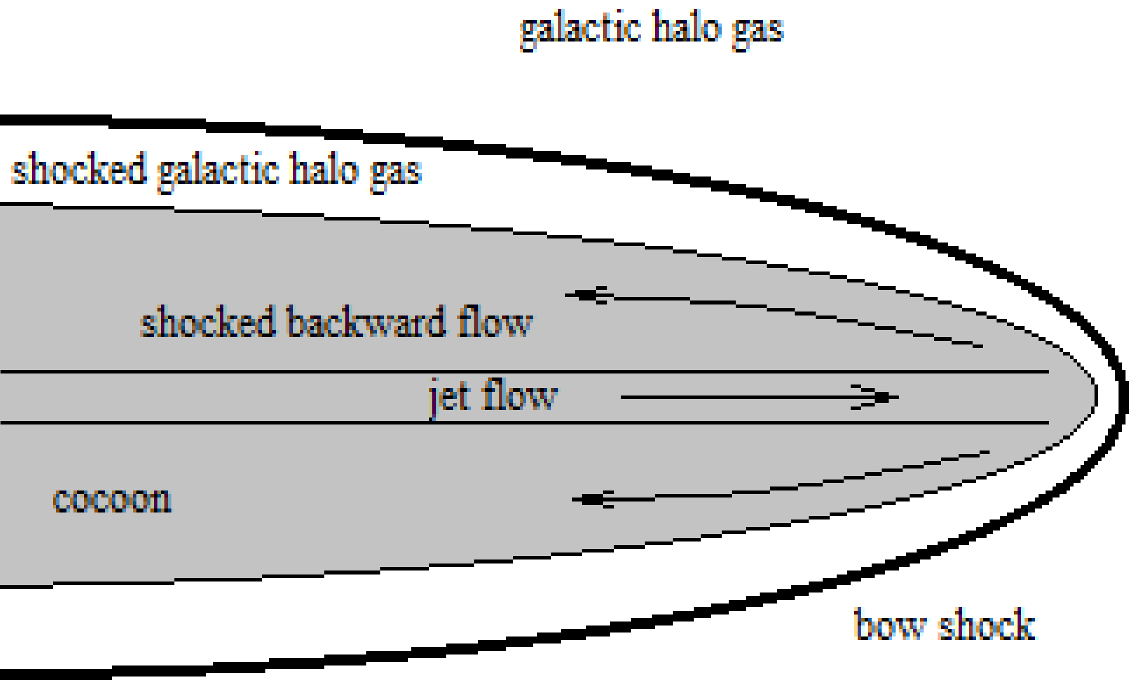

Table 1. Parameters of source components in Andromeda galaxy.

component	γ	$\epsilon_{\max}$	$L_{cr}(z=0)$	$k(A)$
jet	0.5	10^{19} eV	1.3×10^{40} erg s^{-1}	$90\, k_{\odot}(A), A > 4$
bow shock	2.0	5×10^{15} eV	3.2×10^{42} erg s^{-1}	$k_{\odot}(A)A/Z$
cocoon	2.0	6×10^{17} eV	1.4×10^{41} erg s^{-1}	$k_{\odot}(A)A/Z$

Maximum energy of particles accelerated in the jet

$$\epsilon^{j}_{\max} = \mathrm{e}\sqrt{\beta_{\mathrm{j}} L_{\mathrm{mag}} c^{-1}}$$

$$= 1.73 \times 10^{19}\mathrm{eV}\ \beta_{\mathrm{j}}^{1/2} \left(\frac{L_{\mathrm{mag}}}{10^{44}\mathrm{erg\ s^{-1}}}\right)^{1/2}$$

Maximum energy of particles at the bow shock
(3-4 orders lower)

$$\epsilon^{b}_{\max} = \frac{\eta_{\mathrm{esc}}}{2\ln(B/B_b)} \mathrm{e}\sqrt{\beta_{\mathrm{head}} L_{\mathrm{j}} c^{-1}}$$

$$= 1.73 \times 10^{19}\mathrm{eV}\ \frac{\eta_{\mathrm{esc}}}{2\ln(B/B_b)} \beta_{\mathrm{head}}^{1/2} \left(\frac{L_{\mathrm{j}}}{10^{44}\mathrm{erg\ s^{-1}}}\right)^{1/2}$$

Shear acceleration in cylindrical jet with radius *R* and speed *u*

$$\frac{\partial N}{\partial t} = \frac{1}{r}\frac{\partial}{\partial r} rD\frac{\partial N}{\partial r} + \frac{\delta(r-R)}{p^2}\frac{\partial}{\partial p}\frac{u^2}{16c}p^4\frac{\partial N}{\partial p}$$

(sharp boundary of the flow - Berezhko 1982, Jokipii et al. 1989)

Stationary solution for $D \sim D_R(p)r/R$

$$N = N_R(p), r < R, \qquad N = N_R(p)\frac{R}{r}, r > R$$

$$D_R(p)N_R = \frac{1}{p^2}\frac{\partial}{\partial p}\frac{u^2 R}{16c}p^4\frac{\partial N_R}{\partial p}$$

The exact solution for $D_R(p) = \frac{c\lambda(p)}{3} \sim p^2$

$$N_R(p) \sim p^{-3}\left(1 + \sqrt{\frac{16c^2\lambda(p)}{3u^2R}}\right)\exp\left(-\sqrt{\frac{16c^2\lambda(p)}{3u^2R}}\right)$$

Shear acceleration indeed results in the hard energy spectrum of accelerated particles

$$\sim E^{-1}\left(1 + \frac{E}{E_{max}}\right)\exp\left(-\frac{E}{E_{max}}\right)$$

and even harder energy spectrum of run away particles

$$\sim E\left(1 + \frac{E}{E_{max}}\right)\exp\left(-\frac{E}{E_{max}}\right)$$

Features in observable spectrum (PAO 2020)

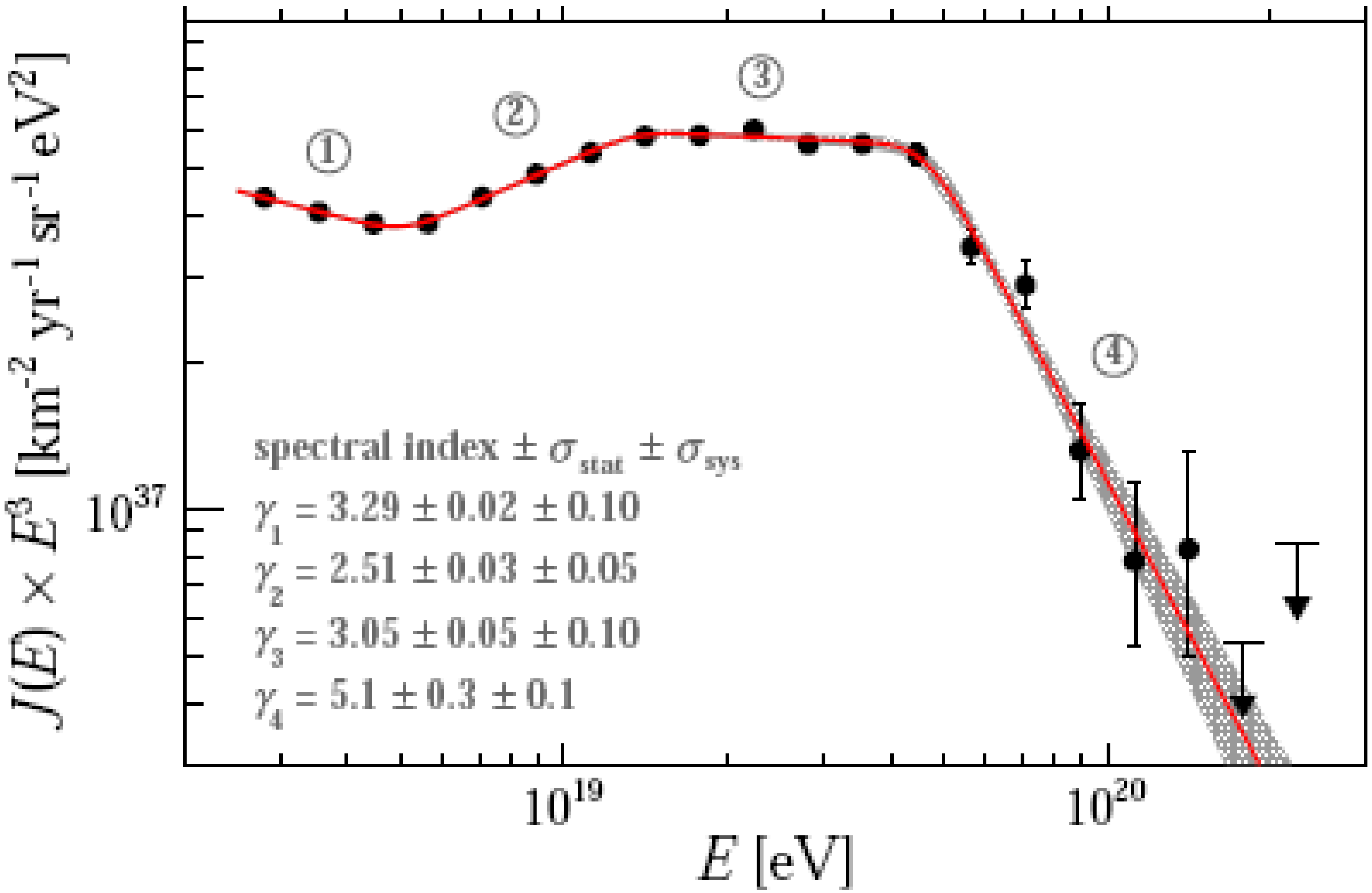

Simpler to explain by one nearby source

Diffusion from the nearby source

$$D = \frac{cl_c}{3}\left(4\frac{E^2}{E_c^2} + 0.9\frac{E}{E_c} + 0.23\frac{E^{1/3}}{E_c^{1/3}}\right), \;\; E_c = ZeBl_c$$

(Harari et al. 2013)

Nearby jets:
galaxy NGC 5128 (Cen A) , 4 Mpc
Black hole mass $5 \cdot 10^7$ solar masses

galaxy M87 in Virgo cluster, 16 Mpc
Black hole mass $6 \cdot 10^9$ solar masses

Nearby supermassive black holes: Galactic Center 8 kpc
$4 \cdot 10^6$ solar masses,
Andromeda galaxy (M31) 800 kpc
$2 \cdot 10^8$ solar masses – both are not active now

Berezinsky et al. (1988) for proton source,
Mollerach & Roulet (2019) for nuclei

Wdowczyk & Wolfendale (1979) for protons

Fermi and eRosita bubbles (Predehl et al. 2020)

Probably related with activity of the central supermassive black hole millions years ago

$W \sim 10^{56}$ erg,
$L \sim 10^{41}$ erg /sec

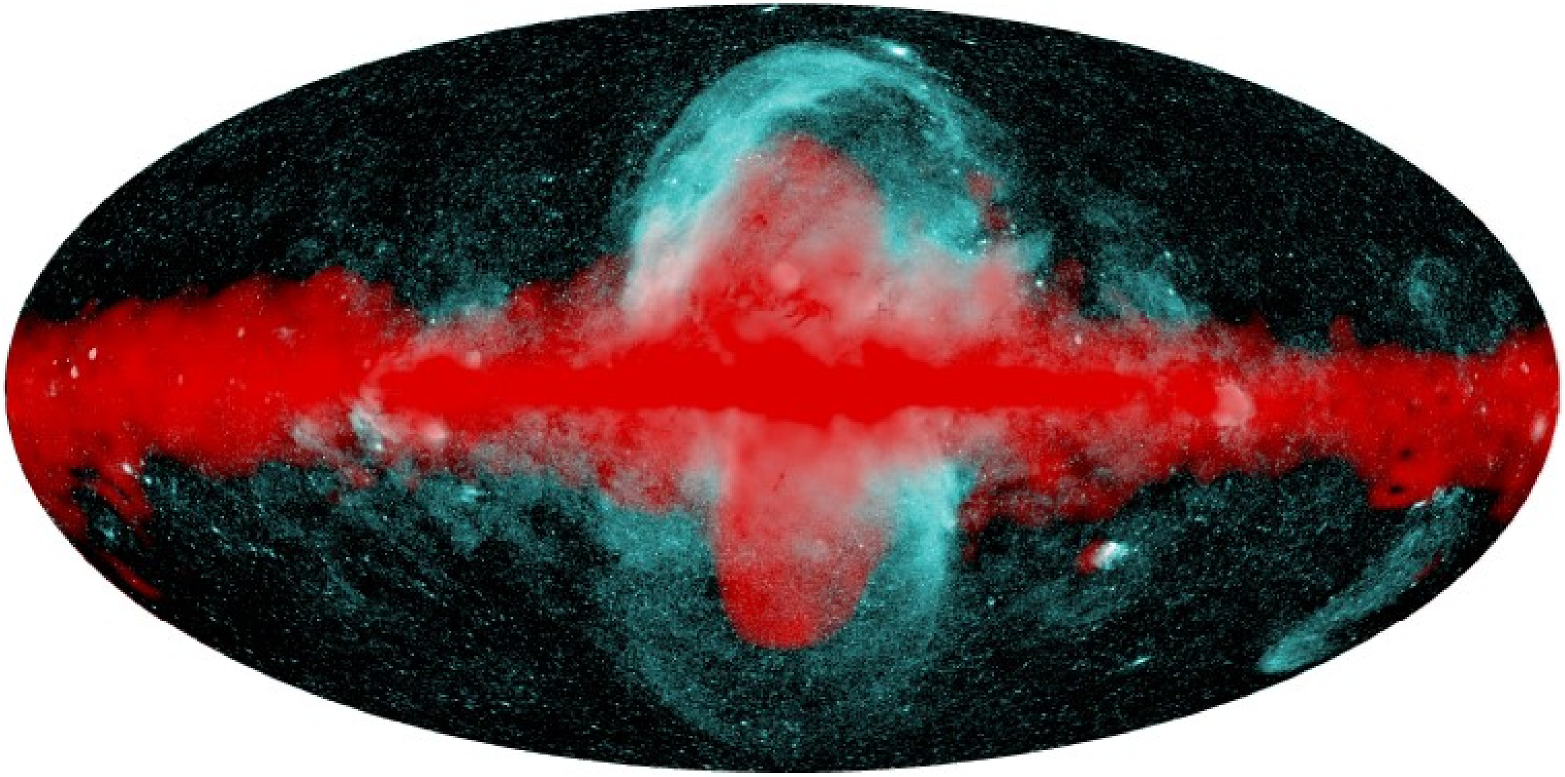

Propagation of protons and nuclei

$$-H(z)(z+1)\frac{\partial N}{\partial z} = \frac{1}{r^2}\frac{\partial}{\partial r}r^2 D(\epsilon, r, z)(z+1)^2\frac{\partial N}{\partial r} + H(z)\epsilon\frac{\partial N}{\partial \epsilon} + \frac{\partial}{\partial \epsilon}b(\epsilon)N$$
$$+4\nu_{ph}(4)N_i(4) + \sum_{A=5}^{56}\nu_{ph}(A)N_i(A) + q(r,\epsilon,z)$$

$$-H(z)(z+1)\frac{\partial N_i(A)}{\partial z} = \frac{1}{r^2}\frac{\partial}{\partial r}r^2 D_i(\epsilon, r, z)(z+1)^2\frac{\partial N_i(A)}{\partial r} + H(z)\epsilon\frac{\partial N_i(A)}{\partial \epsilon} + \frac{\partial}{\partial \epsilon}b(\epsilon)N_i(A)$$
$$-\nu_{ph}(A)N_i(A) + \nu_{ph}(A+1)N_i(A+1) + q_i(r,\epsilon,z)$$

$$H(z) = H_0\sqrt{\Omega_m(1+z)^3 + \Lambda},\ \epsilon = E/A$$

Spectra of protons and nuclei from Andromeda galaxy
(Zirakashvili et al. 2023)

$l_c = 0.13$ Mpc, $B = 10^{-7}$ G, $R = 8$ Mpc, jet every 280 million years, last time – 140 million years ago, mean cosmic ray power - $3 \cdot 10^{42}$ erg/s

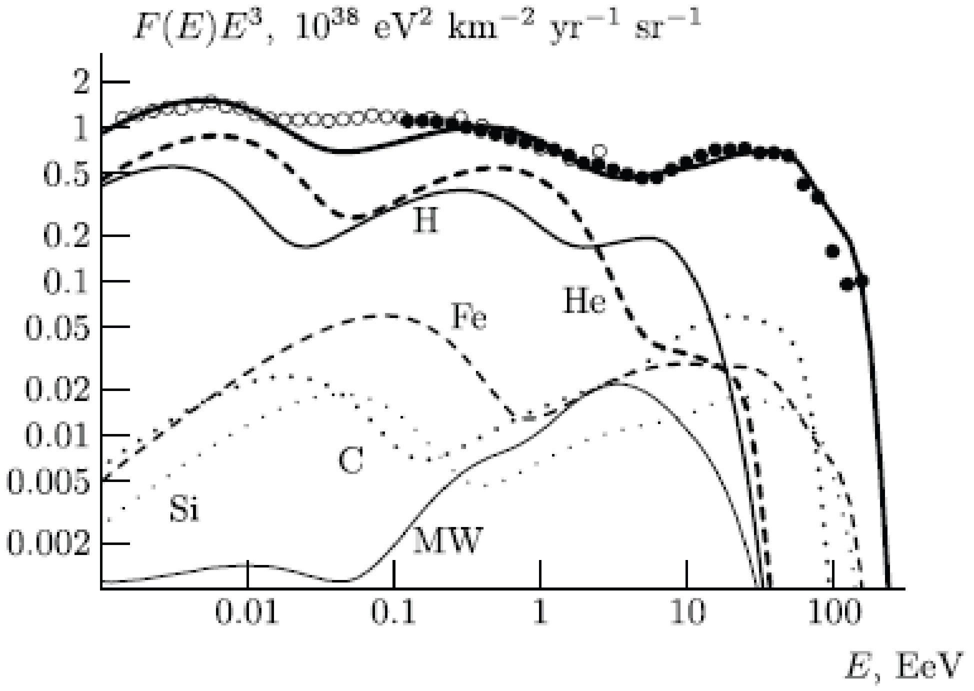

Figure 2. Spectra of different elements and all-particle spectrum (thick solid line) produced in Andromeda galaxy and observed at the Earth position. A possible contribution in the all particle spectrum from the Galactic centre (MW) is shown by the thin solid line. Spectra of Tunka-25, Tunka-133 array (Budnev et al. 2020, open circles) and Pierre Auger Collaboration (2021) (energy shift + 10 per cent, black circles) are also shown.

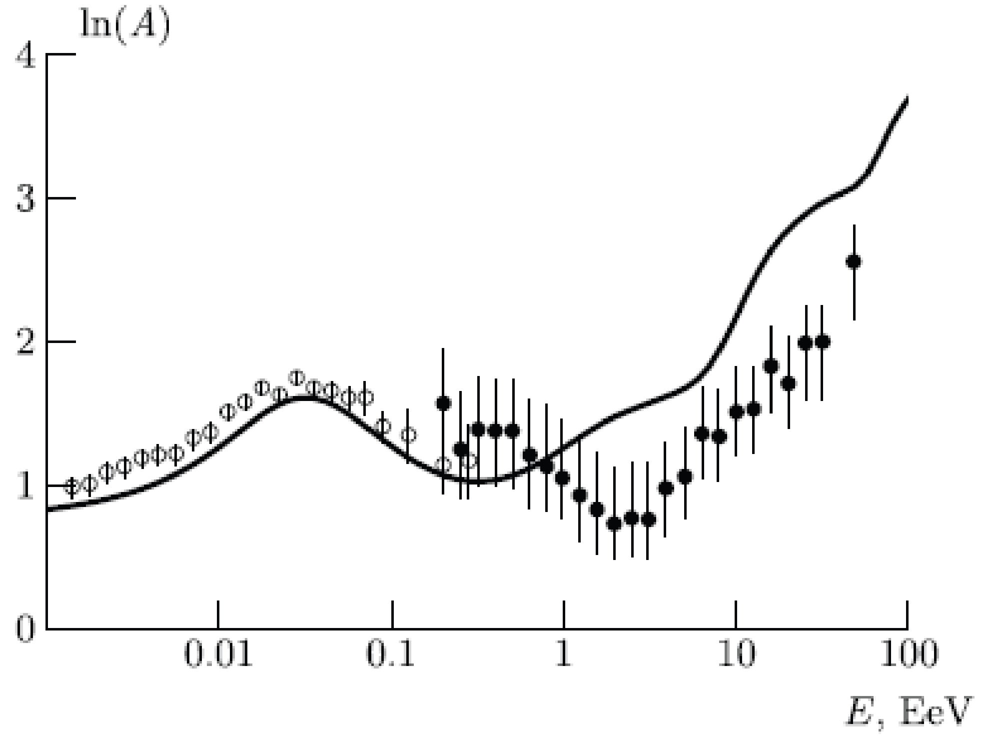

Figure 3. Calculated mean logarithm of atomic number A (solid line). The measurements of Tunka-133, TAIGA-HiSCORE array (Prosin et al. 2022 open circles), and Pierre Auger Collaboration (EPOS-LHC, energy shift + 10 per cent Bellido et al. 2017, black circles) are also shown.

Anisotropy

"hot spot" at 10^{19} eV in the Andromeda direction (Telescope Array Collaboration, Kim et al. 2021)

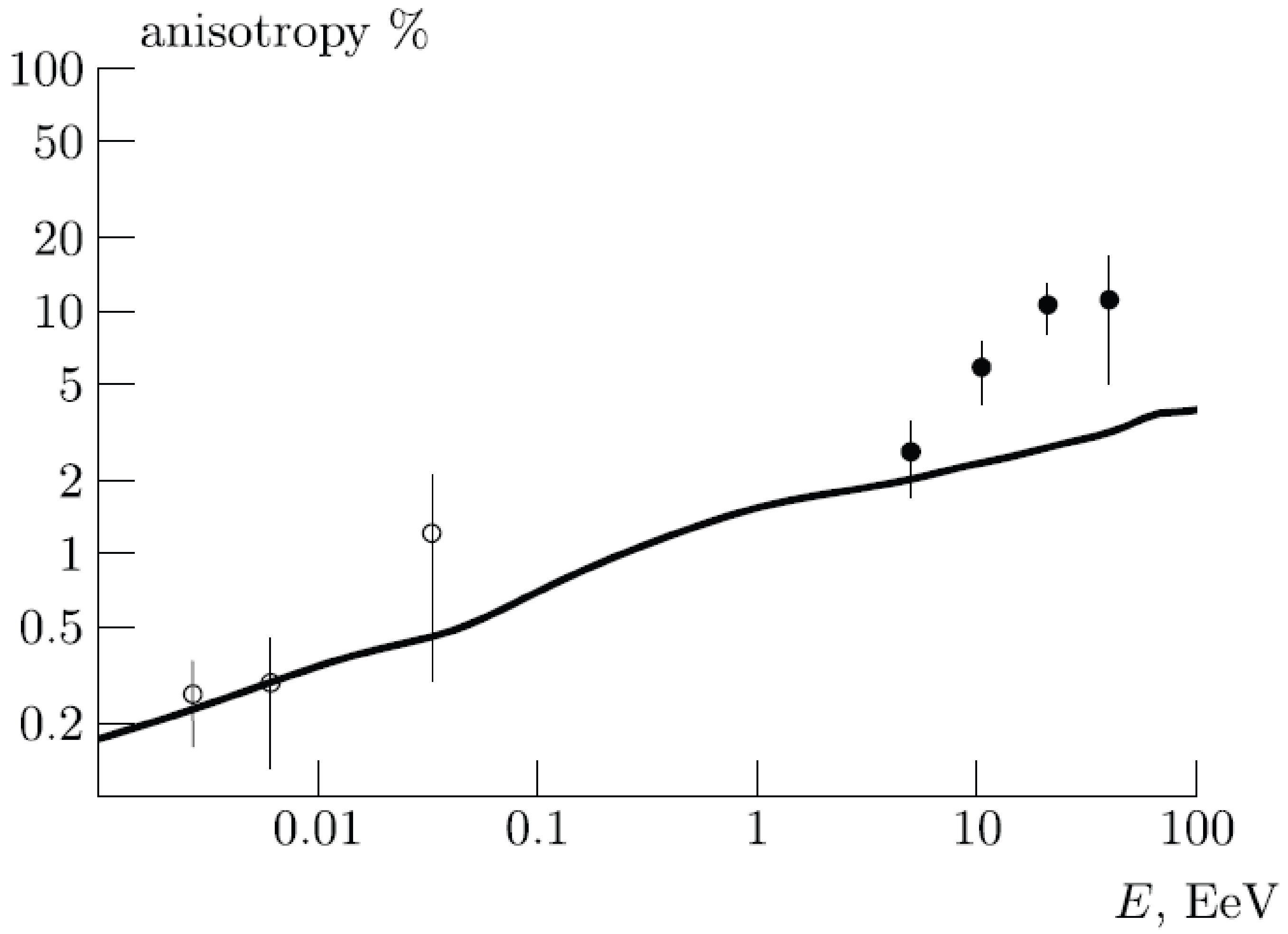

Figure 4. Calculated cosmic ray anisotropy (solid line). The results of Pierre Auger Collaboration (energy shift + 10 per cent, Aab et al. 2018 black circles) and KASCADE-Grande experiment (Chiavassa et al. 2015 open circles) are also shown.

Conclusions

1. Hard spectrum of cosmic ray sources at highest (>EeV) energies inferred from observations is in accordance with the shear acceleration operating in astrophysical jets.
2. Observable spectrum and anisotropy of cosmic rays above 1 PeV can be explained by one nearby flaring source – Andromeda galaxy (M31).

3. Observable PeV cosmic rays are accelerated at the jet bow shock, propagating in galactic halo.

4. Some input in observable spectrum from nearby jets in M87 and Cen A is not excluded.